Earth and Planetary Science Letters 280 (2009) 167–174

Contents lists available at ScienceDirect

Earth and Planetary Science Letters

journal homepage: www.elsevier.com/locate/epsl

Diffusive fractionation of noble gases in mantle with magma channels: Origin of low He/Ar in mantle-derived rocks

Junji Yamamoto [a,b,*], Koshi Nishimura [b], Takeshi Sugimoto [b,c], Keiji Takemura [b], Naoto Takahata [d], Yuji Sano [d]

[a] Woods Hole Oceanographic Institution, Woods Hole, MA 02543, USA
[b] Institute for Geothermal Sciences, Kyoto University, Noguchibaru, Beppu 874-0903, Japan
[c] JMC Geothermal Engineering Co., Ltd., 356-6 Oshimizu, Ogama, Takizawa-mura 020-0151 Japan
[d] Ocean Research Institute, The University of Tokyo, Nakanoku, Tokyo 164-8639, Japan

ARTICLE INFO

Article history:
Received 12 October 2008
Received in revised form 15 January 2009
Accepted 16 January 2009
Available online 13 February 2009

Editor: R.W. Carlson

Keywords:
noble gases
SCLM
diffusive fractionation
magma migration
phenocryst
mantle xenolith

ABSTRACT

By crushing olivine and pyroxene phenocrysts in volcanic rocks from Kyushu Island, Japan, we determined $^3He/^4He$ of 3–7 Ra and $^{40}Ar/^{36}Ar$ of up to 1750. These values are lower than those of MORB. $^4He/^{40}Ar^*$ (down to 0.1) is much lower than the production ratio of $^4He/^{40}Ar^*$ (1–5), where an asterisk denotes correction for the atmospheric contribution. Such values are typical of mantle-derived samples from the island arcs and active continental margins. Although the origin of the low $^3He/^4He$ and $^{40}Ar/^{36}Ar$ of subcontinental mantle has been widely discussed, low $^4He/^{40}Ar^*$ has been given little attention. Actually, $^3He/^4He$ and $^4He/^{40}Ar^*$ of phenocrysts overlap with those of subcontinental mantle xenoliths. Although noble gas compositions of phenocrysts are affected considerably by diffusive fractionation in ascending magma, they have little effect on the noble gases in the mantle xenoliths because it takes 100 years for He/Ar fractionation of ca. 15% for a mantle xenolith with 5 cm diameter. Therefore, the low $^4He/^{40}Ar^*$ of the mantle xenoliths is inferred to result from another kinetic fractionation in the mantle.

During generation and migration of magma in the mantle, lighter noble gases diffuse rapidly out into the magma. This diffusive fractionation can explain low $^4He/^{40}Ar^*$ and somewhat low $^3He/^4He$ in the residual mantle. Furthermore, the combination of the diffusive fractionation and subsequent radiogenic ingrowth explain the fact that data from subcontinental mantle xenoliths have extremely low $^3He/^4He$ and various $^4He/^{40}Ar^*$. Consequently, $^4He/^{40}Ar^*$ and $^3He/^4He$ in mantle-derived materials are proposed as indicators of the degree of noble gas depletion of the source mantle.

1. Introduction

The relative composition of secondary nuclides generated by nuclear reactions converges with the production ratio over time. The production value thereby serves as an initial value to elucidate evolutive processes of the mantle. In fact, $^4He/^{40}Ar^*$ is particularly useful as an indicator for examining consequences of degassing of oceanic basalt, where $^{40}Ar^*$ denotes nonatmospheric ^{40}Ar ($^{36}Ar_{observed}$ $[(^{40}Ar/^{36}Ar)_{observed} - (^{40}Ar/^{36}Ar)_{air}]$). For time scales of 10^8 years or less, the instantaneous $^4He/^{40}Ar^*$ production ratio in mantle is likely to show a constant value of 4–5, depending on the K/U ratio, which is assumed to be 12,000–13,000 (Fig. 1(a)). The accumulated $^4He/^{40}Ar^*$ for several Gyr evolution is expected to be 1–2 (Fig. 1(b)). Therefore, the current mantle is inferred to have $^4He/^{40}Ar^*$ of ca. 1–5. The $^4He/^{40}Ar^*$ in the magma would be elevated because He preferentially diffuses away from crystalline phases in the source mantle into the magma if partial melting or infiltration of exotic magma occurs in the source mantle. Furthermore, He is considerably more soluble than Ar in silicate melts (e.g., Jambon et al., 1986; Carroll and Stolper, 1991; 1993; Shibata et al., 1996; 1998; Nuccio and Paonita, 2000; Guillot and Sarda, 2006), which engenders more extensive degassing of Ar relative to He: the degassing increases the $^4He/^{40}Ar^*$ of residual magma (e.g., Sarda and Graham, 1990; Moreira and Sarda, 2000; Sarda and Moreira, 2002; Burnard, 2004). In this view, it is noted that low $^4He/^{40}Ar^*$ (ca. 0.1) has been reported occasionally for basaltic magma (Honda et al., 1993; Marty et al., 1994; Harrison et al., 2004; Nuccio et al., 2008) and frequently for mantle-derived xenoliths (Poreda and Farley, 1992; Valbracht et al., 1996; Matsumoto et al., 2000; Yamamoto et al., 2004; Buikin et al., 2005; Gautheron et al., 2005; Kim et al., 2005; Hopp et al., 2007). Possible low (U + Th)/K in the source mantle results in low $^4He/^{40}Ar^*$. The instantaneous production ratio of $^4He/^{40}Ar$ is estimated as around 0.5 if (U + Th)/K in the source mantle is one order of magnitude lower than that of MORB. However, we have no evidence of such low (U + Th)/K in mantle-derived rocks. Fig. 2 presents a diagram of $^4He/^{40}Ar^*$ and $^4He/^{21}Ne^*$ for peridotites, where $^{21}Ne^*$ indicates nonatmospheric ^{21}Ne ($^{22}Ne_{observed}$ $[(^{21}Ne/^{22}Ne)_{observed} - (^{21}Ne/^{22}Ne)_{air}]$). Actually, $^4He/^{21}Ne^*$ of the peridotites is correlated with $^4He/^{40}Ar^*$. It is indicative of a significant and systematic elemental fractionation of ^4He from nonatmospheric ^{21}Ne

* Corresponding author. Woods Hole Oceanographic Institution, Woods Hole, MA 02543, USA. Tel.: +1 508 289 3658; fax: +1 508 457 2193.
E-mail address: jyamamoto@whoi.edu (J. Yamamoto).

0012-821X/$ – see front matter © 2009 Elsevier B.V. All rights reserved.
doi:10.1016/j.epsl.2009.01.029

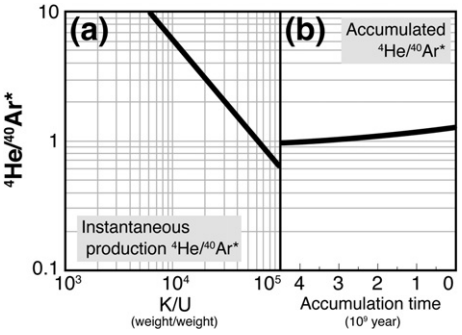

Fig. 1. (a) Instantaneous production ratio of radiogenic He and Ar in an original mantle source with various K/U and uniform Th/U of 3.1. (b) Accumulated production ratio of radiogenic He and Ar in an original mantle source with present K/U of 12,700 and Th/U of 3.1 in weight. In fact, ^{4}He/^{40}Ar* decreases concomitantly with increasing accumulation time because of different decay constants of U and ^{40}K. Actually, MORBs respectively have K/U and Th/U of 12,700 (Jochum et al., 1983) and 3.1 (Staudacher et al., 1989).

and ^{40}Ar (Patterson et al., 1994; Honda and Patterson, 1999) rather than low (U + Th)/K in the source mantle. Gautheron et al. (2005) explained the low ^{3}He/^{36}Ar in mantle xenoliths compared to MORB source by the preferential loss of He from fluid inclusions in mantle xenoliths to the matrix of mineral grains and then to inter-grain spaces. Matsuda and Marty (1995) and Burnard (2004) proposed a similar model by which He can be enriched in melt during partial melting following diffusion from crystalline phases into magma. Complementary residual mantle and magma derived from it are expected to have low ^{4}He/^{40}Ar*. The same diffusive fractionation will occur in phenocrysts in ascending magma (Harrison et al., 2004; Nuccio et al., 2008).

As demonstrated by results of this study, the diffusive loss of a lighter element or isotope from solid phase to melt is a key phenomenon that is useful for tracing pristine chemical and isotopic compositions of mantle-derived materials. Therefore, we test this assumption quantitatively in combination with the influence of subsequent accumulation of radiogenic ^{4}He and ^{40}Ar using published noble gas data for peridotites, phenocrysts, and ocean island basalts along with newly obtained noble gas data on phenocrysts in volcanic rocks from Japan.

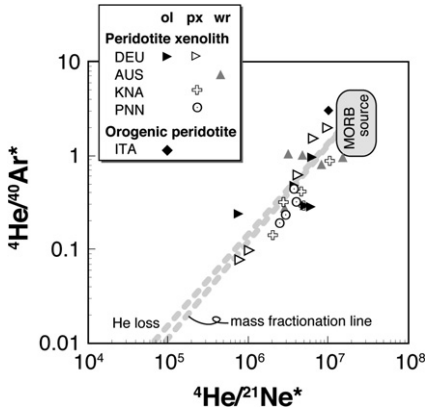

Fig. 2. ^{4}He/^{40}Ar* versus ^{4}He/^{21}Ne* diagram of data obtained from peridotites with crushing experiments, where * indicates correction for atmospheric contamination. Data sources are as follows: peridotite xenoliths from Germany (DEU) (Buikin et al., 2005; Gautheron et al., 2005), Australia (AUS) (Matsumoto et al., 2000), Kenya (KNA) (Hopp et al., 2007), and Pannonian (PNN) (Buikin et al., 2005); orogenic peridotites from Italy (ITA) (Matsumoto et al., 2005). Data with ^{21}Ne/^{22}Ne and ^{40}Ar/^{36}Ar of less than 0.03 and 320, respectively, are not shown. Actually, ^{21}Ne can be generated nucleogenically from (α, n) reaction on ^{18}O and (n, α) reaction on ^{24}Mg (Wetherill, 1954). The ^{4}He/^{21}Ne* production ratio in the mantle is estimated as 2.2×10^7 (Yatsevich and Honda, 1997; Leya and Wieler, 1999). The ^{4}He/^{21}Ne* of the lithosphere is determined primarily by its chemical composition, which is unlikely to change dramatically between reservoirs. Therefore, the ^{4}He/^{21}Ne* of the mantle is likely to be constant, as is true for ^{4}He/^{40}Ar*.

2. Samples

Samples analyzed in this study are phenocrystic olivine and pyroxenes in volcanic rocks from Kyushu Island, Japan (Table 1 and Fig. 3). Kyushu Island has two main volcanic lines: a volcanic front and a volcanic line along with the Beppu–Shimabara graben (Fig. 3). Samples from Kirishima volcanoes (Karakuni-dake, Shinmoe-dake, Ohachi and Takachiho-dake) represent the volcanic front. As representatives from the Beppu–Shimabara graben, we collected volcanic rocks from Kinpo-san and Atago-yama. Volcanoes of Oninomi, Yufu-dake, Komezuka, and Tateno-lava are situated on the intersection of two volcanic lines. Olivine and pyroxenes in the present volcanic rocks are euhedral and not zoned. The average grain size differs among samples, but 0.5 mm diameter is typical.

3. Experimental method

Noble gases were extracted from fresh olivine and pyroxenes by vacuum crushing. Olivine and pyroxenes are retentive for noble gases; in-situ addition of radiogenic ^{4}He and ^{40}Ar is quite small because of the very low contents of U, Th, and K in such minerals. Furthermore, the in-situ post eruptive addition of ^{4}He and ^{40}Ar has little effect on the original isotopic compositions of samples with young eruption ages (<ca. 1 Ma: Table 1). The crushing method is thought to be effective for extracting noble gases trapped in fluid or melt inclusions, which contain only small amounts of in-situ generated nuclides (e.g., Kurz, 1986; Graham et al., 1992a,b). Recently there have been reports, however, of cosmogenic nuclides released by crushing (Scarsi, 2000; Yokochi et al., 2005; Moreira and Madureira, 2005). We consider that such an effect has a negligible influence on these results because most samples were collected from a cliff with a steep gradient, where the surrounding trees' growth implied that cliff failure had occurred within 100 years. Other samples were collected from lava cave, quarry, and mudslide deposits.

Before vacuum crushing, mineral grains were preheated at 150 °C in vacuum for 8 h. During crushing, extracted gases were exposed to a cold trap at liquid N_2 temperature to remove gases that had adsorbed onto newly created powder surfaces. Helium analyses were performed using a sector-type mass spectrometer (Helix SFT; GV Instruments Ltd.) installed at Ocean Research Institute (ORI), the University of Tokyo, which is equipped with a conventional quadrupole mass spectrometer for analysis of argon isotopic composition. Sensitivities and isotopic ratios for He and Ar were calibrated using an artificial helium standard gas (HESJ) with ^{3}He/^{4}He of 20.63 ± 0.10 Ra (Matsuda et al., 2002) and diluted air standard, where Ra stands for atmospheric ^{3}He/^{4}He. Procedural crushing blanks for ^{4}He and ^{40}Ar were, respectively, less

Table 1
Sample descriptions.

Sample	Volcano	No. on map	Sampling site	Eruption age	Reference
onn02	Oninomi-lava	1	Cliff	10 ka	Ohta et al. (1992)
onn03	Oninomi-lava	1	Cliff	10 ka	Ohta et al. (1992)
yf11	Yufu-dake	2	Steep gradient	<6.3 ka	Hoshizumi et al. (1988)
kmz01	Komezuka	3	Lava cave	<2.7 ka	Kobayashi et al. (1999)
ttn01	Tateno-lava	4	Cliff	25–73 ka	Kobayashi et al. (1999)
kp01	Kinpo-san	5	Cliff	0.54 Ma	Toshida et al. (2006)
atg01	Atago-yama	6	Quarry	1.1 Ma	Nakada and Kamata (1988)
kkd01	Karakumi-dake	7	Mud slide	18–15 ka	Imura and Kobayashi (2001)
smd01	Shinmoe-dake	8	Steep gradient	15–6.3 ka	Imura and Kobayashi (2001)
ohc01	Ohachi	9	Cliff	1923 A.D.	Imura and Kobayashi (2001)
tkc01	Takachino-dake	10	Cliff	6.3 ka	Imura and Kobayashi (2001)

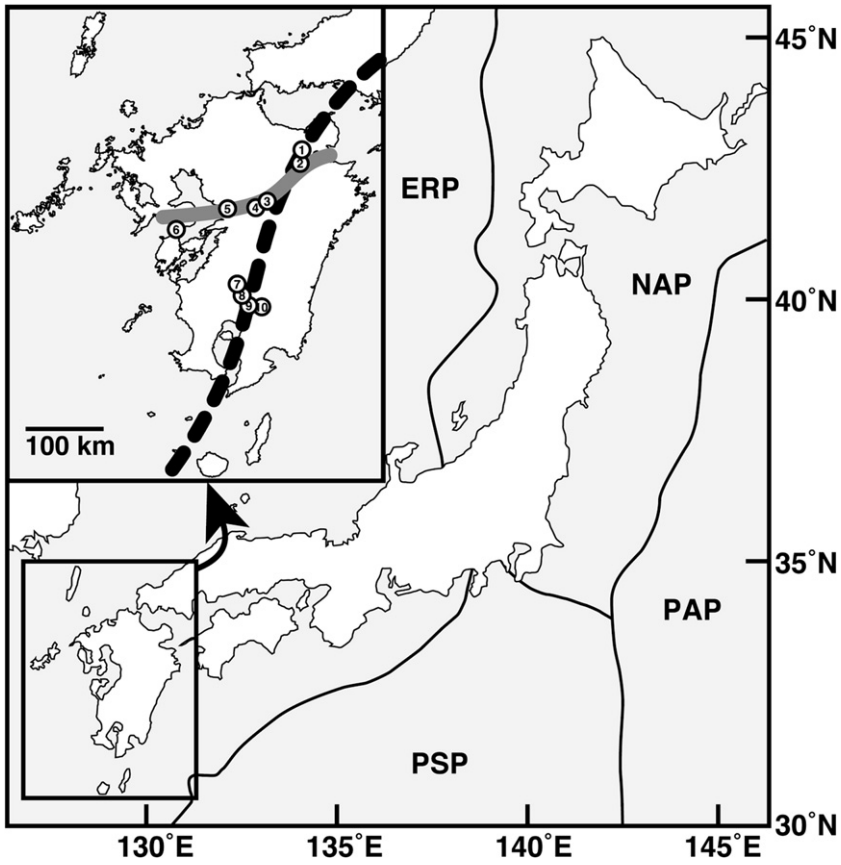

Fig. 3. Schematic map showing the location of Kyushu Island, Japan and sampling points. The broken line shows a volcanic front. The solid line shows the Beppu–Shimabara graben. On the map, ERP, NAP, PAP, and PSP respectively represent the Eurasia Plate, North America Plate, Pacific Plate, and Philippine Sea Plate.

than 3.0×10^{-10}, 4×10^{-9} cm^3 STP. Analytical conditions for noble gases at the ORI were described in an earlier report (Sano et al., 2008).

4. Results

Table 2 presents noble gas isotope results. The ^{3}He/^{4}He of the present samples are mostly between a typical MORB value (8.75 ± 2.14 Ra: Graham, 2002) and a recommended value for Sub-Continental Lithospheric Mantle (SCLM) (6.1 ± 0.9 Ra: Gautheron and Moreira, 2002). Argon isotopic ratios (^{40}Ar/^{36}Ar) are higher than those for air (295.5) but much lower than the MORB values, which are often up to 10,000 and sometimes as high as 40,000 (Burnard et al., 1997). Overall ^{40}Ar/^{36}Ar of pyroxenes are lower than those of olivine, especially for sample yf11, which might indicate a larger fraction of atmospheric argon in the pyroxenes, which crystallize after olivine. The ^{4}He/^{40}Ar* varies between 0.11 and 1.2 which is much lower than the production ratio of 1–5.

Table 2
Noble gas isotopic compositions of phenocrysts from Kyushu volcanos, Japan.

Sample	Mineral	Weight (g)	^{4}He (10^{-9})	^{40}Ar(10^{-8})	^{3}He/^{4}He(Ra)	^{40}Ar/^{36}Ar	^{4}He/^{40}Ar*
onn02	Olivine	1.105	175.879	33.9	6.959 ± 0.040	1.749 ± 100	0.625 ± 0.052
onn03	Pyroxene	1.520	56.314	32.19	6.968 ± 0.046	781.0 ± 9.1	0.281 ± 0.006
yf11	Olivine	1.348	20.879	3.214	7.231 ± 0.097	634 ± 29	1.22 ± 0.12
yf11	Cpx	0.844	*	2.866	*	338.7 ± 9.3	*
ttn01	Cpx	0.903	*	2.003	*	352 ± 15	*
kmz01	Olivine	0.560	4.185	2.485	6.98 ± 0.24	417 ± 23	0.58 ± 0.12
kmz01	Cpx	1.133	*	1.517	*	363 ± 15	*
atg01	Olivine	1.305	1.790	6.726	6.21 ± 0.28	385.9 ± 6.5	0.114 ± 0.008
kp01	Olivine	0.354	*	4.908	*	569 ± 40	*
smd01	Opx	0.826	1.126	6.837	5.23 ± 0.31	331.7 ± 6.2	0.151 ± 0.026
kkd01	Opx	0.858	0.549	4.844	*	308.3 ± 5.5	0.27 ± 0.12
kkd01	Cpx	1.064	0.967	1.667	7.06 ± 0.36	354 ± 18	0.35 ± 0.11
ohc01	Opx	1.001	*	3.007	*	309.0 ± 6.9	*
ohc01	Cpx	0.885	*	1.905	*	379 ± 30	*
tkc01	Opx	1.022	1.395	25.00	3.01 ± 0.14	292.8 ± 5.6	*
tkc01	Cpx	0.996	0.667	2.241	*	323 ± 13	0.35 ± 0.16

N.B., Unit for abundance is cm^3 STP/g. *: not measured. ^{40}Ar* is ^{40}Ar corrected for atmospheric contamination.
Experimental uncertainties in amounts are generally within 10%.

As the origin of Unzen volcano, which is represented by Atago-yama, constituting the Beppu–Shimabara graben, an OIB-like hotspot has been proposed, based on trace element compositions and distance from the volcanic front (Nakada and Kamata, 1991; Sugimoto et al., 2005). No appreciable difference in the noble gas compositions was found between the samples from two volcanic lines in Kyushu Island. Helium isotopic compositions of these samples reflect that the magma was derived from a source resembling MORB or SCLM rather than OIB.

5. Discussion

5.1. Occurrence of low $^4He/^{40}Ar^*$ in the mantle reservoir

If the relative composition of the parental radioactive nuclides is known, the production ratio of radiogenic–nucleogenic nuclides such as ^4He, ^{21}Ne and ^{40}Ar can be predicted. A noble gas isotopic characteristic of the present phenocrysts is low $^4He/^{40}Ar^*$ (0.11–1.2) compared to the production ratio (1–5). It is difficult to explain the low $^4He/^{40}Ar^*$ of the phenocrysts by elemental fractionation that occurs during crystallization in ascending magma because the noble gases are likely to have similar incompatibilities in major upper mantle mineral phases. Moreover, they are not fractionated relative to one another during melting and crystallization involving olivine, clinopyroxene, and orthopyroxene (Baxter et al., 2007; Heber et al., 2007). Mainly, we extracted noble gases from melt inclusions in phenocrysts using crushing experiments. Noble gas compositions of the host phenocryst have little effect on those of the melt inclusion. Consequently, it is not necessary to consider the solubility-controlled noble gas fractionation in the phenocryst matrix.

Both elemental fractionation by degassing of ascending magma, and magmatic assimilation with wall rock are important to discuss the chemical composition of magma, which is captured as melt inclusions in the phenocrysts. Magmatic degassing will increase $^4He/^{40}Ar^*$ and $^4He/^{21}Ne^*$ in residual magma because of the higher solubility of He relative to Ne and Ar. Furthermore, assimilation with wall rock, whose isotopic composition converges to a radiogenic one over time, is expected to render magma more radiogenic, which is not observed. Therefore, we infer that the low $^4He/^{40}Ar^*$ of the phenocrysts does not result from either mechanism.

Peridotite xenoliths from Samoa and Kerguelen show low $^4He/^{40}Ar^*$ (Poreda and Farley, 1992; Valbracht et al., 1996). Moreira and Sarda (2000) discussed the origin of the low $^4He/^{40}Ar^*$ as follows. Vesiculation processes at oceanic islands result from Rayleigh distillation (Moreira and Sarda, 2000). In the early stage of degassing, the distillation process generates small vesicles with $^4He/^{40}Ar^*$ that are lower than that of primary magma. The early evolved vesicles might have been stored in mineral interfaces or grain boundaries in the lithospheric mantle around Samoa and Kerguelen (Moreira and Sarda, 2000) when the ocean island magma percolates through the lithospheric mantle. Regarding phenocrysts, they might trap the early evolved vesicles during crystallization. This is not, however, sufficient to explain all data of phenocrysts with low $^4He/^{40}Ar^*$. The phenocrysts from Japan show melt inclusions with the constant vesicle/melt volume ratio, indicating that the vesicles are shrinkage bubbles formed by exsolution of volatiles from the melt in the inclusion on cooling, not the trapped vesicles. In addition, $^4He/^{40}Ar^*$ of the phenocrysts show a positive relation with $^3He/^4He$ (Fig. 4), which is not explained by entrapment of the early evolved vesicles.

Harrison et al. (2004) and Nuccio et al. (2008) proposed that the low $^3He/^4He$ of phenocrysts is explainable by diffusive fractionation of He from the phenocrysts in ascending magma. When ascending magma degases after crystallization of phenocrysts, lighter noble gases in the phenocrysts preferentially diffuse into the magma, leading to lowering of $^4He/^{21}Ne^*$, $^4He/^{40}Ar^*$, and $^3He/^4He$ of the phenocrysts. Herein, we shall only briefly outline the timescale to change the $^4He/^{40}Ar^*$ and $^3He/^4He$ in phenocrysts because diffusive

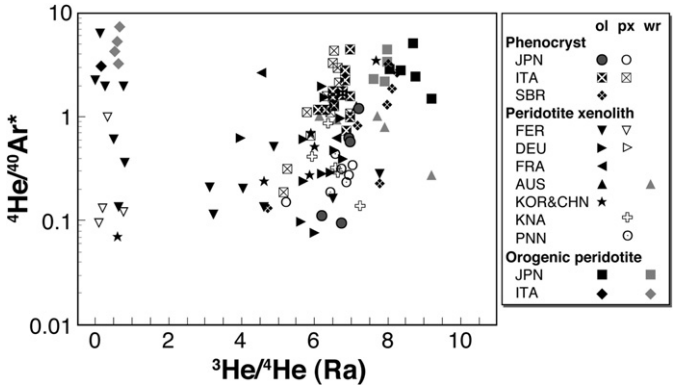

Fig. 4. $^3He/^4He$ versus $^4He/^{40}Ar^*$ diagram of phenocrysts from quaternary volcanoes in Kyushu island, Japan (JPN) with data obtained by crushing mantle-derived materials. Data sources are as follows: phenocrysts from Italy (ITA) (Marty et al., 1994; Nuccio et al., 2008); phenocrysts from Siberia, Russia (SBR) (Harrison et al., 2004); peridotite xenoliths from Far Eastern Russia (FER) (Yamamoto et al., 2004), Germany (DEU) (Buikin et al., 2005; Gautheron et al., 2005), France (FRA) (Gautheron et al., 2005), Australia (AUS) (Matsumoto et al., 2000), Korea (KOR), China (CHN) (Kim et al., 2005), Kenya (KNA) (Hopp et al., 2007) and Pannonian (PNN) (Buikin et al., 2005); orogenic peridotites from Japan (JPN) (Matsumoto et al., 2001), and Italy (ITA) (Matsumoto et al., 2005).

fractionation is described further in the following section. When diffusive fractionation occurs at 1200 °C, assuming a grain size of 1 mm for a phenocrystic olivine, it takes six months to reduce $^3He/^4He$ and $^4He/^{40}Ar^*$ from 8 Ra and 3 to 5.4 Ra and 0.1, respectively. It seems reasonable to presume that the low $^3He/^4He$ and $^4He/^{40}Ar^*$ of phenocrysts are attributable to the diffusive loss of lighter noble gases from the phenocrysts in ascending magma. Both $^3He/^4He$ and $^4He/^{40}Ar^*$ of the mantle peridotites overlap considerably with those of the phenocrysts (Fig. 4), indicating that the diffusive fractionation also affects the mantle peridotites. However, it takes more than 100 years to reduce $^4He/^{40}Ar^*$ from 3 to 2.5 for mantle xenoliths with 5 cm diameter. During that interval, $^3He/^4He$ of 8 Ra drops only to 7.7 Ra. This phenomenon requires some further explanation. Another possibility for the low $^4He/^{40}Ar^*$ of the mantle peridotites is to assume that kinetic fractionation occurs in the source mantle. All noble gases are incompatible in olivine and pyroxenes. Large amounts of all noble gases can be partitioned into magma during partial melting or magma infiltration. The higher diffusivity of helium than those of other noble gases might engender fractionation of $^4He/^{40}Ar^*$. Burnard (2004) modeled noble gas diffusion out of the bulk mantle into fast diffusion pathways (such as fractures or melt channels) during mantle melting. Results of that study suggest that He/Ar fractionation of one order of magnitude occurs in the primary melt if fast diffusion channels are spaced several meters apart and if the noble gas residence time is of approximately days to weeks. Complementary He in the residual mantle will be depleted preferentially: when magma migrates through the source mantle, $^4He/^{40}Ar^*$ in the source mantle is expected to decrease. Mantle peridotites and magma that had originated from the source mantle are expected to have low $^4He/^{40}Ar^*$. To test this perspective, we computed the diffusive fractionation in mantle with magma channels, particularly on the assumption of a subduction-related environment.

5.2. Diffusive fractionation

Noble gases are partitioned preferentially into magma because of their high incompatibilities when magma infiltrates into the mantle or is generated in mantle. Considerable elemental fractionation is likely to result from a nonequilibrium condition because of their rapid diffusion at mantle temperature and pressure. However, the relative diffusivities of noble gases in mantle minerals are not known. For

example, if diffusivity is governed by vacancy diffusion mechanisms, the relative diffusivities of elements a and b can be expressed as

$$\frac{D_a}{D_b} \approx \sqrt{\frac{M_b}{M_a}}, \tag{1}$$

where D is the diffusion coefficient and M is the atomic mass. Examples of the relative diffusivity of noble gases are D_{3He}/D_{4He} of 1.15 and D_{4He}/D_{40Ar} of 3.16. Therefore, $^4He/^{40}Ar$ decreases concomitantly with decreasing contents of ^4He and ^{40}Ar in the residual mantle, which is also true for $^4He/^{21}Ne^*$ and $^3He/^4He$.

Herein, for simplicity, we consider the diffusion of an element or isotope in mantle bounded by two parallel planar magma channels. The following diffusion equations govern the compositional profile:

$$\frac{\partial C}{\partial t} = D\frac{\partial^2 C}{\partial x^2}, \tag{2}$$

$$\text{wherein} \quad C = C_i, \text{ when } t = 0 \text{ and } 0 \le x \le 2l, \tag{3}$$

$$\text{and} \quad C = C_f, \text{ when } t > 0, \; x = 0 \text{ and } x = 2l. \tag{4}$$

In those equations, C is the concentration of the element, l is the half width between the magma channels, C_i is the initial concentration of the element in mantle, and C_f is the constant concentration of the element in the magma. The solution of Eqs. (2)–(4) is obtainable as

$$\frac{C - C_f}{C_i - C_f} = \frac{4}{\pi}\sum_{n=1}^{\infty}\frac{1}{n} exp\left[-\left(\frac{n\pi}{2l}\right)^2 Dt\right] \sin\frac{n\pi x}{2l} \quad (n = 1, 3, 5\cdots). \tag{5}$$

For this study, we simply assumed that C_f is zero. Using Eq. (5), we calculated the diffusion profile of a target element in a source mantle bounded by two parallel planar magma channels (Fig. 5). The diffusive fractionation in the source mantle depends on the diffusion coefficient, timescale and channel spacing. Fig. 6 portrays the predicted fractionation of $^4He/^{40}Ar^*$ and contents of ^4He and ^{40}Ar as functions of the timescale and channel spacing when diffusive fractionation occurs at 1200 °C. Although we do not know the channel

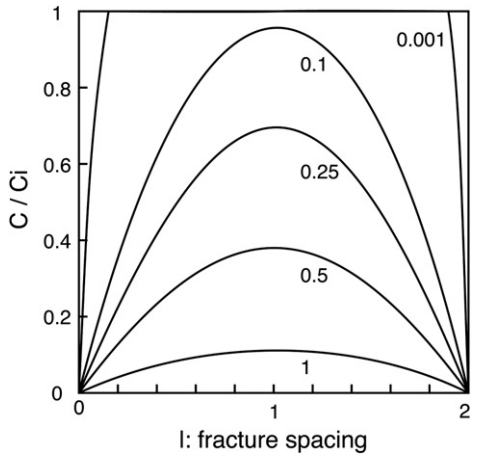

Fig. 5. Predicted diffusion profiles of noble gases in a mantle region based on a model of diffusive noble gas fractionation during partial melting or infiltration of magma. Initially, noble gases are distributed homogeneously throughout the mantle. Fast diffusion paths for the noble gases (such as fractures or melt channels) are emplaced some distance ($2l$) apart. Noble gases diffuse from the solid into fast diffusion channels (melt) during time t, after which the noble gases are removed progressively from the system. Diffusion profiles are calculated using Eq. (5). The numbers with the profiles represent the Fo value ($=D\times t/2l$), where D, t, and l respectively signify the diffusion coefficient, time and half fracture spacing. For example, the Fo value of 0.1 corresponds to $D = 1\times10^{-10}$ cm^2/s; $l = 0.5$ cm; $t = 30$ years. In addition, C_i and C respectively represent the initial concentrations of noble gases and the concentration at time t.

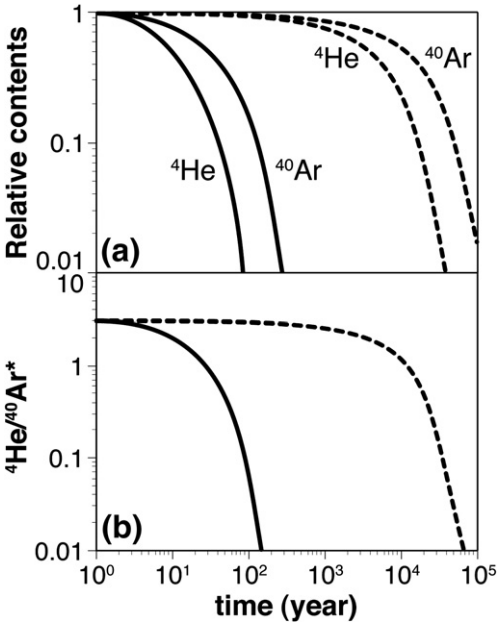

Fig. 6. Averaged relative contents of (a) ^4He and ^{40}Ar, and (b) $^4He/^{40}Ar$ as functions of time and fracture spacing. Solid and broken lines represent the diffusive fractionation with fracture spacing of 1 cm and 20 cm, respectively. The fractionation trajectories are governed by D_a (D_a = (diffusivity of a)). The calculation is based on $D_{4He} = 1.61\times10^{-10}$ cm^2/s in olivine at 1200 °C (Trull and Kurz, 1993) and $D_{4He}/D_{40Ar} = 3.16$ estimated from Eq. (1).

spacing in the mantle beneath the active continental margins and island arcs, channel spacing observed in an orogenic peridotite body ranges from several millimeters to several meters; furthermore, their abundance increases concomitantly with decreased channel spacing (Takazawa et al., 1999). Assuming channel spacings of 20 cm and 1 cm, it takes 17 and 0.05 Ka, respectively, to produce one order of magnitude lower ^4He content. In the interval, $^4He/^{40}Ar^*$ of 3 drop respectively to 0.7 and 0.5. Similarly, $^3He/^4He$ decrease from 8.0 Ra to 6.0 and 5.6 Ra, respectively. Volcanoes at the active continental margins and island arcs typically have a life span of 20–40 Ka (Tomiya, 1991). Therefore, when subduction-related magma passes continuously through the mantle, dramatic decreases in $^4He/^{40}Ar^*$ and $^3He/^4He$ in the source mantle are quite conceivable. In the next section, we verify whether this calculation can explain noble gas isotopic compositions of mantle materials derived from the active continental margins and island arcs.

5.3. Quantitative test for low $^4He/^{40}Ar^*$ and $^3He/^4He$

The shaded area in Fig. 7 depicts the change in noble gas isotopic compositions of a source mantle fractionated by the diffusive loss. Data with $^3He/^4He$ more than 4 Ra are explainable by diffusive ^4He–^{40}Ar and ^3He–^4He fractionation. However, the data are apparently distributed on a curve with an inclination that is steeper than the theoretical diffusive trajectories (shaded area). The dark gray broken line is the best fitting exponential curve to the datasets. The fitting curve closely approximates a diffusive fractionation trajectory with $D_{3He}/D_{4He} = 1.05$. It is noteworthy that Trull and Kurz (1993) reported low D_{3He}/D_{4He} of 1.09 ± 0.04 for olivine and 1.04 ± 0.04 for pyroxene in comparison with the relative diffusivity of 1.15 calculated from Eq. (1). We mentioned in passing that they used natural mantle minerals as diffusion media, which have CO_2 inclusions involving He. The He in the minerals is expected to first leave the inclusions before diffusing in the mineral matrix, which might cause slow He diffusivity. Nevertheless, this is not a determining cause of the low D_{3He}/D_{4He} because low D_{3He}/D_{4He} of 1.03 was reported from gem-quality fluorapatite that was free of fluid inclusions (Shuster et al., 2003). Trull and Kurz (1993) described several possible causes of the low D_{3He}/D_{4He}, for example,

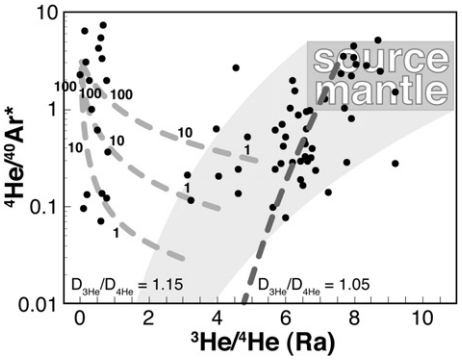

Fig. 7. $^3He/^4He$ versus $^4He/^{40}Ar^*$ diagram of subcontinental mantle peridotites. Data are from Fig. 4. The shaded area shows a trend of the diffusive noble gas fractionation from the source mantle (gray rectangle) using D_{3He}/D_{4He} of 1.15 and D_{4He}/D_{40Ar} of 3.16. A dark gray broken line is the best-fitting exponential curve to sets of data with $^3He/^4He$ of more than 4 Ra, which corresponds to the diffusion curve with D_{3He}/D_{4He} of 1.05. Light gray broken lines show the radiogenic change of the depleted mantle, which originally has $^3He/^4He$ of 3.1, 4.1, and 5.2 Ra and $^4He/^{40}Ar^*$ of 0.03, 0.1, and 0.3, respectively. The radiogenic change is based on an original source mantle with K/U of 12 700 and Th/U of 3.1, in which K, Th, and U contents are presumed to be unaffected by the depletion. Numbers labeling the broken lines denote the elapsed time (kiloyear).

diffusion mechanisms involving correlation of successive atomic jumps, temporal coupling of the diffusing atom and host crystal movements, and vibrational energy quantization for light atoms such as helium. Although the low D_{3He}/D_{4He} for mantle minerals is not supported by independent evidence, low D_{3He}/D_{4He} was reported for basaltic glass (1.10 ± 0.03 at 1000 °C: Trull and Kurz, 1999) and quartz (1.00 ± 0.05: Shuster and Farley, 2005). Assuming D_{3He}/D_{4He} of 1.05, we can estimate an unfractionated $^3He/^4He$ of SCLM to be 7.7 ± 1.8 Ra for given $^4He/^{40}Ar^*$ of 3 (Fig. 7), which includes the value of 6.1 ± 0.9 Ra proposed as a representative of SCLM by Gautheron and Moreira (2002), but which resembles that of MORB. The data scatter around the fitting line, which might reflect mantle-source heterogeneity. As described previously, much study remains to be done to elucidate diffusion coefficients of noble gases in mantle minerals. Accumulation of experimental data will support a more rigorous discussion of the diffusive fractionation and heterogeneity of $^3He/^4He$ in mantle.

The fractionated mantle is expected to be depleted considerably in He during production of about one order of magnitude lower $^4He/^{40}Ar^*$ (Fig. 6). In this case, radiogenic ^4He induces changes in $^3He/^4He$ and $^4He/^{40}Ar^*$. We simulated time-integrated effects of the radiogenic ^4He and ^{40}Ar on $^3He/^4He$ and $^4He/^{40}Ar^*$ in the depleted mantle. The light-gray broken lines in Fig. 7 toward the upper left from halfway on the diffusive fractionation lines represent the time-integrated effect on radiogenic nuclides. Data with extremely low $^3He/^4He$ and various $^4He/^{40}Ar^*$ are explainable by the radiogenic effect. In the case of residual mantle with $^4He/^{40}Ar^*$ of 0.3 and 0.1, it takes 50 and 9 Ka to fall to less than 1 Ra, respectively, indicating that $^3He/^4He$ in mantle with magma channels decreases rapidly. This probably explains why few data having 1–3 Ra are reported. Consequently, the wide distribution of $^4He/^{40}Ar^*$ and $^3He/^4He$ of the subcontinental mantle-derived materials is explainable by a combination of diffusive fractionation related to magmatic migration and subsequent radiogenic ingrowth.

5.4. $^4He/^{40}Ar^*$: an index to mantle depletion

The $^3He/^4He$ of the subduction-related SCLM and arc mantle are more variable than that of MORB (Fig. 4). A recent study of He isotopes in Proterozoic SCLM xenoliths from western Europe (Gautheron et al., 2005) showed low and uniform $^3He/^4He$ (6.32 ± 0.39 Ra). Gautheron et al. (2005) discuss two models to explain the low and uniform $^3He/^4He$. The first model is that the SCLM beneath western Europe was invaded by recent and local metasomatic fluid having $^3He/^4He$ of ca. 6 Ra. Another model is that metasomatism occurs globally throughout the entire SCLM, where $^3He/^4He$ is kept constant by balance of ^3He derived from asthenosphere with radiogenic ^4He. Both models necessitate mantle metasomatism related to a U-rich component. It would be acceptable as a mantle process especially for mantle beneath active continental margins and island arcs, where subduction-related fluid infiltrates continuously through intergranular area in the source mantle. Indeed melt inclusions with high U contents have been observed in a far eastern Russian mantle xenolith with extremely low $^3He/^4He$ where the far eastern Asia area was located at a subduction zone in the Mesozoic Era (Yamamoto et al., in press).

However, correlation between $^4He/^{40}Ar^*$ and $^3He/^4He$ cannot be explained merely by the invasion of a U-rich component and subsequent radiogenic ingrowth. The introduction of the diffusive fractionation might reveal various aspects of the cause of wide variation of $^3He/^4He$ and $^4He/^{40}Ar^*$ in SCLM. The low $^4He/^{40}Ar^*$ of mantle-derived materials indicates depletion of noble gases in the source mantle. Moreover, subduction-related fluid having a considerable amount of U generates a source mantle with very low $^3He/U$, leading to extremely low $^3He/^4He$, as observed in the far eastern Asian mantle. Perhaps for that reason, the SCLM partly shows low $^3He/^4He$ compared to MORB. Therefore, diffusive fractionation accompanied by invasion of melt with various U contents might be useful as a geochemical signature to differentiate the SCLM at active continental margins. The fundamental assumption that the SCLM traps fluid with low $^3He/^4He$ (Yamamoto et al., 2004; Gautheron et al., 2005) remains convincing. The diffusive fractionation serves as another mechanism to interpret noble gas features of the SCLM properly, especially for low $^4He/^{40}Ar^*$.

The diffusive fractionation model requires a prior melting event that depletes the mantle source region. High $^4He/^{40}Ar^*$ might be shown complementarily in magma at an early stage of volcanism if the diffusive fractionation plays a major role in low $^4He/^{40}Ar^*$ in the mantle. However, it is difficult to distinguish the effect of the diffusive fractionation from that of solubility-controlled fractionation during magmatic degassing.

It is possible to apply diffusive fractionation to trace the origin of low $^4He/^{40}Ar^*$ in oceanic island basalt (OIB) and oceanic peridotite xenoliths. Low $^4He/^{40}Ar^*$ of the oceanic peridotite xenoliths might result from the trapping of early evolved vesicles during percolation of oceanic island magma (Moreira and Sarda, 2000). The diffusive fractionation process is also a valid explanation of the low $^4He/^{40}Ar^*$ as follows. The source mantle is partly depleted in lighter noble gases if OIB magma is originated from successive partial melting of a source mantle. The noble gas compositions of the OIB magma must be depleted in lighter noble gases with development of volcanism if a sequence of an OIB volcanism is derived from the same part of a source mantle. Similarly, the low $^4He/^{40}Ar^*$ of the oceanic peridotite xenoliths might represent depletion of lighter noble gases in oceanic lithospheric mantle because of extraction of MORB magma. This is a reason why the OIB and the oceanic peridotite xenoliths show a correlation between $^4He/^{40}Ar^*$ and $^4He/^{21}Ne^*$ (e.g. Graham, 2002), as observed in the SCLM. Accordingly, kinetic fractionation might alter our perspective of mantle processes.

6. Conclusions

From volcanic rocks from Kyushu Island, Japan, we obtained phenocrystic olivine and pyroxenes with low $^4He/^{40}Ar^*$ and $^3He/^4He$ compared to those of MORB-source. The present results show no systematic difference from published data of subarc and subcontinental mantle materials. Overall, the $^3He/^4He$ of the subarc and subcontinental mantle are roughly separable into two regimes: data with $^3He/^4He$ more than 3 Ra and less than 1 Ra. The $^3He/^4He$ of the former samples have a positive correlation with $^4He/^{40}Ar^*$. Although the correlation for phenocrysts is explainable by the diffusive loss of lighter noble gases from the phenocrysts in ascending magma, such a process has little effect on the noble gases in mantle xenoliths because of their larger size. Possibly, the correlation for the mantle xenoliths results from diffusive fractionation accompanied by magma migration in the mantle. The

diffusive fractionation engenders depletion in noble gases in the source mantle. Therefore, the effect of radiogenic addition on the residual mantle is large. Such a rapid radiogenic ingrowth engenders extremely low $^3He/^4He$ (<1 Ra) and various $^4He/^{40}Ar^*$, as occasionally reported for subcontinental mantle-derived xenoliths. Assuming this concept to be true, $^3He/^4He$ and $^4He/^{40}Ar^*$ provide useful indices for tracking mantle evolution.

Acknowledgements

We appreciate constructive reviews from Dr. P. Sarda and an anonymous reviewer. We gratefully acknowledge helpful discussions with M.D. Kurz on several points of the paper. We appreciate K. Kiyota for his assistance in analyzing noble gases. H. Ishibashi and N. Hirano afforded us assistance with collecting samples. This study was financially supported in part by Research Fellowships of the Japan Society for the Promotion of Science (JSPS) for Young Scientists and Research Abroad to J. Y.

References

Baxter, E.F., Asimow, P.D., Farley, K.A., 2007. Grain boundary partitioning of Ar and He. Geochim. Cosmochim. Acta 71, 434–451.
Buikin, A., Trieloff, M., Hopp, J., Althaus, T., Korochantseva, E., Schwarz, W.H., Altherr, R., 2005. Noble gas isotopes suggest deep mantle plume source of late Cenozoic mafic alkaline volcanism in Europe. Earth Planet. Sci. Lett. 230, 143–162.
Burnard, P.G., 2004. Diffusive fractionation of noble gases and helium isotopes during mantle melting. Earth Planet. Sci. Lett. 220, 287–295.
Burnard, P., Graham, D., Turner, G., 1997. Vesicle-specific noble gas analyses of "popping rock": implications for primordial noble gases in Earth. Science 276, 568–571.
Carroll, M.R., Stolper, E.M., 1991. Argon solubility and diffusion in silica glass: implications for the solution behavior of molecular gases. Geochim. Cosmochim. Acta 55, 211–225.
Carroll, M.R., Stolper, E.M., 1993. Noble gas solubilities in silicate melts and glasses: new experimental results for argon and the relationship between solubility and ionic porosity. Geochim. Cosmochim. Acta 57, 5039–5051.
Gautheron, C., Moreira, M., 2002. Helium signature of the subcontinental lithospheric mantle. Earth Planet. Sci. Lett. 199, 39–47.
Gautheron, C., Moreira, M., Allègre, C., 2005. He, Ne and Ar composition of the European lithospheric mantle. Chem. Geol. 217, 97–112.
Graham, D.W., 2002. Noble gas isotope geochemistry of mid-ocean ridge and ocean island basalts: characterization of mantle source reservoirs. Reviews in Mineralogy and Geochemistry 47 (Noble Gases in Geochemistry and Cosmochemistry Edited by Porcelli, D., Ballentine, C. J., Wieler, R.). The Mineralogical Society of America, Washington, DC, pp. 247–317.
Graham, D.W., Humphris, S.E., Jenkins, W.J., Kurz, M.D., 1992a. Helium isotope geochemistry of some volcanic rocks from Saint Helena. Earth Planet. Sci. Lett. 110, 121–131.
Graham, D.W., Jenkins, W.J., Schilling, J.-G., Thompson, G., Kurz, M.D., Humphris, S.E., 1992b. Helium isotope geochemistry of mid-ocean ridge basalts from the South Atlantic. Earth Planet. Sci. Lett. 110, 133–147.
Guillot, B., Sarda, P., 2006. The effect of compression on noble gas solubility in silicate melts and consequences for degassing at mid-ocean ridges. Geochim. Cosmochim. Acta 70, 1215–1230.
Harrison, D., Barry, T., Turner, G., 2004. Possible diffusive fractionation of helium isotopes in olivine and clinopyroxene phenocrysts. Eur. J. Mineral. 16, 213–220.
Heber, V.S., Brooker, R.A., Kelley, S.P., Wood, B.J., 2007. Crystal-melt partitioning of noble gases (helium, neon, argon, krypton, and xenon) for olivine and clinopyroxene. Geochim. Cosmochim. Acta 71, 1041–1061.
Honda, M., Patterson, D.B., 1999. Systematic elemental fractionation of mantle-derived helium, neon, and argon in mid-oceanic ridge glasses. Geochim. Cosmochim. Acta 63, 2863–2874.
Honda, M., McDougall, I., Patterson, D.B., Doulgeris, A., Clague, D.A., 1993. Noble gases in submarine pillow basalt glasses from Loihi and Kilauea, Hawaii: a solar component in Earth. Geochim. Cosmochim. Acta 57, 859–874.
Hopp, J., Trieloff, M., Altherr, R., 2007. Noble gas compositions of the lithospheric mantle below the Chyulu Hills volcanic field, Kenya. Earth Planet. Sci. Lett. 261, 635–648.
Hoshizumi, H., Ono, K., Mimura, K., Noda, T., 1988. Geology of the Beppu district. Quadrangle Series of Geological Survey of Japan Fukuoka, vol. (14) 75. GSJ, Ibaraki, p. 137.
Imura, R., Kobayashi, T., 2001. Geological map of Kirishima volcano. AIST-GSJ, Geological Map of Volcanoes, No. 11.
Jambon, A., Weber, H.W., Braun, O., 1986. Solubility of He, Ne, Ar, Kr, and Xe in a basalt melt in the range 1250–1600. Geochemical implications. Geochim. Cosmochim. Acta 50, 401–408.
Jochum, K.P., Hofmann, A.W., Ito, E., Seufert, H.M., White, W.M., 1983. K, U and Th in mid-ocean ridge basalt glasses and heat production, K/U and K/Rb in the mantle. Nature 306, 431–436.
Kim, K.H., Nagao, K., Tanaka, T., Sumino, H., Nakamura, T., Okuno, M., Lock, J.B., Youn, J.S., Song, J., 2005. He–Ar and Nd–Sr isotopic compositions of ultramafic xenoliths and host alkali basalts from the Korean peninsula. Geochem. J. 39, 341–356.
Kobayashi, T., Tameike, T., Uto, K., 1999. Aso central volcanic cones. Catalog of Quaternary Volcanoes in Japan.
Kurz, M.D., 1986. Cosmogenic helium in a terrestrial igneous rock. Nature 320, 435–439.
Leya, I., Wieler, R., 1999. Nucleogenic production of Ne isotopes in Earth's crust and upper mantle induced by alpha particles from the decay of U and Th. J. Geophys. Res. 104, 15439–15450.
Marty, B., Trull, T., Lussiez, P., Tanguy, J.C., 1994. He, Ar, O, Sr and Nd isotope constraints on the origin and evolution of Mount Etna magmatism. Earth Planet. Sci. Lett. 126, 23–39.
Matsuda, J., Marty, B., 1995. The $^{40}Ar/^6Ar$ ratio of the undepleted mantle; a reevaluation. Geophys. Res. Lett. 22, 1937–1940.
Matsuda, J., Matsumoto, T., Sumino, H., Nagao, K., Yamamoto, J., Miura, Y., Kaneoka, I., Takahata, N., Sano, Y., 2002. The $^3He/^4He$ ratio of the new internal He standard of Japan (HESJ). Geochem. J. 36, 191–195.
Matsumoto, T., Honda, M., McDougall, I., O' Reilly, S.Y., Norman, M., Yaxley, G., 2000. Noble gases in pyroxenites and metasomatised peridotites from the Newer Volcanics, southeastern Australia: implications for mantle metasomatism. Chem. Geol. 168, 49–73.
Matsumoto, T., Chen, Y., Matsuda, J., 2001. Concomitant occurrence of primordial and recycled noble gases in the Earth's mantle. Earth Planet. Sci. Lett. 185, 35–47.
Matsumoto, T., Morishita, T., Matsuda, J., Fujioka, T., Takebe, M., Yamamoto, K., Arai, S., 2005. Noble gases in the Finero phlogopite–peridotites, western Italian Alps. Earth Planet. Sci. Lett. 238, 130–145.
Moreira, M., Sarda, P., 2000. Noble gas constraints on degassing processes. Earth Planet. Sci. Lett. 176, 375–386.
Moreira, M., Madureira, P., 2005. Cosmogenic helium and neon in 11 Myr old ultramafic xenoliths: consequences for mantle signatures in old samples. Geochem. Geophys. Geosyst. 6, Q08006. doi:10.1029/2005GC000939.
Nakada, S., Kamata, H., 1988. Petrogenetical relationship of basalts and andesites in southern part of the Shimabara peninsula, Kyushu, Japan. Bull. Volcanol. Soc. Jpn. 33, 273–289.
Nakada, S., Kamata, H., 1991. Temporal change in chemistry of magma source under Central Kyushu, Southwest Japan: progressive contamination of mantle wedge. Bull. Volcanol. 53, 182–194.
Nuccio, P.M., Paonita, A., 2000. Investigation of the noble gas solubility in H_2O–CO_2 bearing silicate liquids at moderate pressure II: the extended ionic porosity (EIP) model. Earth Planet. Sci. Lett. 183, 499–512.
Nuccio, P.M., Paonita, A., Rizzo, A., Rosciglione, A., 2008. Elemental and isotope covariation of noble gases in mineral phases from Etnean volcanics erupted during 2001–2005, and genetic relation with peripheral gas discharges. Earth Planet. Sci. Lett. 272, 683–690.
Ohta, T., Hasenaka, T., Ban, M., Sasaki, M., 1992. Characteristic geology and petrology of non-arc type volcanism at Oninomi monogenetic volcano, Yufu-Tsurumi graben. Bull. Volcanol. Soc. Jpn. 37, 119–131.
Patterson, D.B., Honda, M., McDougall, I., 1994. Noble gases in mafic phenocrysts and xenoliths from New Zealand. Geochim. Cosmochim. Acta 58, 4411–4427.
Poreda, R.J., Farley, K.A., 1992. Rare gases in Samoan xenoliths. Earth Planet. Sci. Lett. 113, 129–144.
Sano, Y., Tokutake, T., Takahata, N., 2008. Accurate measurement of atmospheric helium isotopes. Anal. Sci. 24, 521–525.
Sarda, P., Graham, D., 1990. Mid-ocean ridge popping rocks: implications for degassing at ridge crests. Earth Planet. Sci. Lett. 97, 268–289.
Sarda, P., Moreira, M., 2002. Vesiculation and vesicle loss in mid-ocean ridge basalt glasses: He, Ne, Ar elemental fractionation and pressure influence. Geochim. Cosmochim. Acta 66, 1449–1458.
Scarsi, P., 2000. Fractional extraction of helium by crushing of olivine and clinopyroxene phenocrysts: effects on the $^3He/^4He$ measured ratio. Geochim. Cosmochim. Acta 64, 3751–3762.
Shibata, T., Takahashi, E., Matsuda, J., 1996. Noble gas solubility in binary CaO–SiO_2 system. Geophys. Res. Lett. 23, 3139–3142.
Shibata, T., Takahashi, E., Matsuda, J., 1998. Solubility of neon, argon, krypton, and xenon in binary and ternary silicate systems: a new view on noble gas solubility. Geochim. Cosmochim. Acta 62, 1241–1253.
Shuster, D.L, Farley, K.A., Sisterson, J.M., Burnett, D.S., 2003. Quantifying the diffusion kinetics and spatial distributions of radiogenic ^4He in minerals containing proton-induced ^3He. Earth Planet. Sci. Lett. 217, 19–32.
Shuster, D.L., Farley, K.A., 2005. Diffusion kinetics of proton-induced ^{21}Ne, ^3He, and ^4He in quartz. Geochim. Cosmochim. Acta 69, 2349–2359.
Staudacher, T., Sarda, P., Richardson, S.H., Allègre, C.J., Sagna, I., Dmitriev, L.V., 1989. Noble gases in basalt glasses from a Mid-Atlantic Ridge topographic high at 14′N: geodynamic consequences. Earth Planet. Sci. Lett. 96, 119–133.
Sugimoto, T., Ishibashi, H., Wakamatsu, S., Yanagi, T., 2005. Petrologic evolution of Pre-Unzen and Unzen magma chambers beneath the Shimabara Peninsula, Kyushu, Japan: evidence from petrography and bulk rock chemistry. Geochem. J. 39, 241–256.
Takazawa, E., Frey, F.A., Shimizu, N., Saal, A., Obata, M., 1999. Polybaric petrogenesis of mafic layers in the Horoman peridotite complex, Japan. J. Petrol. 40, 1827–1851.
Tomiya, A., 1991. Volume of mantle diapir compatible with life span of a typical island-arc volcano. Bull. Volcanol. Soc. Jpn. 36, 211–221.
Toshida, K., Uto, K., Matsumoto, A., 2006. K–Ar dating of Kimpo volcano, Northern Ryukyu arc. Bull. Volcanol. Soc. Jpn. 51, 31–40.
Trull, T.W., Kurz, M.D., 1993. Experimental measurements of ^3He and ^4He mobility in olivine and clinopyroxene at magmatic temperatures. Geochim. Cosmochim. Acta 57, 1313–1324.
Trull, T.W., Kurz, M.D., 1999. Isotopic fractionation accompanying helium diffusion in basaltic glass. J. Mol. Struct. 485–486, 555–567.

Valbracht, P.J., Honda, M., Matsumoto, T., Mattielli, N., McDougall, I., Ragettli, R., Weis, D., 1996. Helium, neon and argon isotope systematics in Kerguelen ultramafic xenoliths: implications for mantle source signatures. Earth Planet. Sci. Lett. 138, 29–38.

Wetherill, G.W., 1954. Variations in the isotopic abundances of neon and argon extracted from radioactive minerals. Phys. Rev. 96, 679–683.

Yamamoto, J., Kaneoka, I., Nakai, S., Kagi, H., Prikhod'ko, V.S., Arai, S., 2004. Evidence for subduction-related components in the subcontinental mantle from low $^{3}He/^{4}He$ and $^{40}Ar/^{36}Ar$ ratio in mantle xenoliths from Far Eastern Russia. Chem. Geol. 207, 237–259.

Yamamoto, J., Nakai, S., Nishimura, K., Kaneoka, I., Kagi, H., Sato, K., Okumura, T., Prikhod'ko, V.S., Arai, S., in press. Intergranular trace elements in mantle xenoliths from Russian Far East: an example for mantle metasomatism by hydrous melt. The Island Arc. doi:10.1111/j.1440-1738.2008.00642.x.

Yatsevich, I., Honda, M., 1997. Production of nucleogenic neon in the Earth from natural radiogenic decay. J. Geophys. Res. 102 (B5), 10291–10298.

Yokochi, R., Marty, B., Pik, R., Burnard, P., 2005. High $^{3}He/^{4}He$ ratios in peridotite xenoliths from SW Japan revisited: evidence for cosmogenic ^{3}He released by vacuum crushing. Geochem. Geophys. Geosyst. 6. doi:10.1029/2004GC000836.